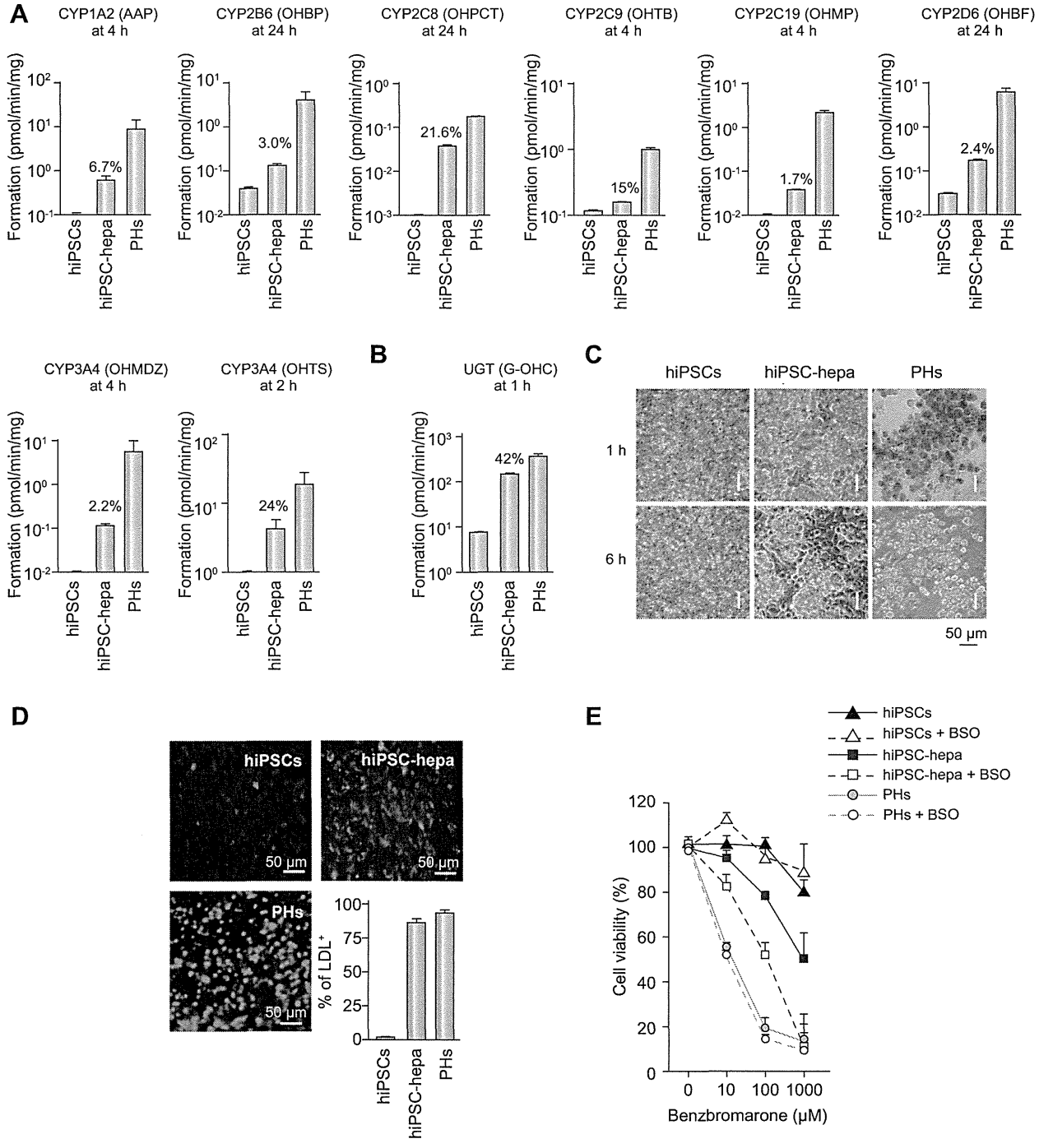

Fig. 4. Evaluation of the drug metabolism capacity and hepatic transporter activity of hiPSC-hepa. hiPSCs (Dotcom) were differentiated into hepatocytes as described in Fig. 2A. (A and B) Quantitation of metabolites in hiPSCs, hiPSC-hepa, and PHs, which were cultured for 48 h after the cells were plated, was examined by treating nine substrates (Phenacetin, Bupropion, Paclitazel, Tolbtamide, *S*-mephenytoin, Bufuralol, Midazolam, Testosterone, and Hydroxyl coumarin; these compounds are substrates for CYP1A2, 2B6, 2C8, 2C9, 2C19, 2D6, 3A4, 3A4 (A) and UGT (B), respectively), and then supernatants were collected at the indicated time. The quantity of metabolites (Acetaminophen [AAP], Hydroxybupropion [OHBP], 6α-hydroxypaclitaxel [OHPCT], Hydroxytolbutamide [OHTB], 4′-hydroxymephenytoin [OHMP], 1′-hydroxybufuralol [OHBF], 1′-hydroxymidazolam [OHMDZ], 6β-hydroxytestosterone [OHTS], 7-Hydroxycoumarin glucuronide [G-OHC], respectively) was measured by LC-MS/MS. The ratios of the activity levels in hiPSC-hepa to the activity levels in PHs rate are indicated in the graph. (C) hiPSCs, hiPSC-hepa, and PHs were examined for their ability to take up ICG (top) and release it 6 h thereafter (bottom). (D) hiPSCs, hiPSC-hepa, and PHs were cultured with medium containing Alexa-Flour 488-labeled LDL (green) for 1 h, and immunohistochemistry was performed. Nuclei were counterstained with DAPI (blue). The percentage of LDL-positive cells was also measured by FACS analysis. (E)

(ALB, CYP2D6, alpha-1-antitrypsin [αAT], CYP3A4, and CYP7A1) increased (Fig. 2C). Hepatic gene expression levels (Supplementary Fig. 6A), amount of ALB secretion (Supplementary Fig. 6B), and CYP2C9 activity level (Supplementary Fig. 6C) of Ad-FOXA2- and Ad-HNF1α-transduced cells were significantly higher than those of Ad-SOX17-, Ad-HEX-, and Ad-HNF4α-transduced cells. These results indicated that FOXA2 and HNF1α transduction promotes more efficiently hepatic differentiation than SOX17, HEX, and HNF4α transduction.

Characterization of the hESC-hepa/hiPSC-hepa

As we have previously reported [6], hepatic differentiation efficiency differs among hESC/hiPSC lines. Therefore, it is necessary to select a hESC/hiPSC line that is suitable for hepatic maturation in the case of medical applications such as drug screening. In the present study, two hESC lines and five hiPSCs lines were differentiated into hepatocyte-like cells, and then their gene expression levels of *ALB* (Fig. 3A) and *CYP3A4* (Supplementary Fig. 7A), and their CYP3A4 activities (Supplementary Fig. 7B) were compared. These data suggest that the iPSC line, Dotcom [11,12], was the most suitable for hepatocyte maturation. To examine whether the iPSC (Dotcom)-hepa has enough hepatic functions as compared with PHs, the amount of albumin (ALB) secretion (Fig. 3B) and the percentage of ALB-positive cells (Fig. 3C) were measured on day 20. The amount of ALB secretion in hiPSC-hepa was similar to that in PHs and the percentage of ALB-positive cells was approximately 90% in iPSC-hepa. We also confirmed that the gene expression levels of CYP enzymes (Fig. 3D), conjugating enzymes (Fig. 3E), hepatic transporters (Fig. 3F), and hepatic nuclear receptors (Fig. 3G) in hiPSC-hepa were similar to those of PHs, although some of them were still lower than those of PHs. Because the gene expression level of the fetal CYP isoform, *CYP3A7*, in hiPSC-hepa was higher than that of PHs, mature hepatocytes and hepatic precursors were still mixed. We have previously confirmed that Ad vector-mediated gene expression in the hepatoblasts (day 9) continued until day 14 and almost disappeared on day 18 [7]. Therefore, the hepatocyte-related genes expressed in hiPSC-hepa are not directly regulated by exogenous FOXA2 or HNF1α. Taken together, endogenous hepatocyte-related genes in hiPSC-hepa should have been upregulated by FOXA2 and HNF1α transduction.

To further confirm that hiPSC-hepa have sufficient levels of hepatocyte functions, we evaluated the ability of urea secretion (Fig. 3H) and glycogen storage (Supplementary Fig. 8). The amount of urea secretion in hiPSC-hepa was about half of that in PHs. HiPSC-hepa exhibited abundant storage of glycogen. Because CYP1A2, 2B6, and 3A4 are involved in the metabolism of a significant proportion of the currently available commercial drugs, we tested the induction of *CYP1A2*, *2B6*, and *3A4* by chemical stimulation (Fig. 3I). *CYP1A2*, *2B6*, and *3A4* are induced by β-naphthoflavone [bNF], phenobarbital [PB], or rifampicin [RIF], respectively. Although undifferentiated hiPSCs did not respond to either bNF, PB, or RIF (data not shown), hiPSC-hepa produced more metabolites in response to chemical stimulation, suggesting that inducible CYP enzymes were detectable in hiPSC-hepa (Fig. 3I). However, the induction potency of *CYP1A2*, *2B6*, and *3A4* in hiPSC-hepa were lower than that in PHs.

Drug metabolism capacity and hepatic transporter activity of hiPSC-hepa

Because metabolism and detoxification in the liver are mainly executed by CYP enzymes, conjugating enzymes, and hepatic transporters, it is important to assess the function of these enzymes and transporters in hiPSC-hepa. Among the various enzymes in liver, CYP1A2, 2B6, 2C8, 2C9, 2C19, 2D6 and 3A4, UGT are the important phase I and II enzymes responsible for metabolism. Nine substrates, Phenacetin, Bupropion, Paclitazel, Tolbtamide, S-mephenytoin, Bufuralol, Midazolam, Testosterone, and Hydroxyl coumarin, which are the substrates of CYP1A2, 2B6, 2C8, 2C9, 2C19, 2D6, 3A4, 3A4 (Fig. 4A), and UGT (Fig. 4B), respectively, were used to estimate the drug metabolism capacity of hiPSC-hepa compared with that of PHs. To precisely estimate the drug metabolism capacity, the amounts of metabolites were measured during the phase when production of metabolites was linear (Supplementary Fig. 9). These results indicated that our hiPSC-hepa have the capacity to metabolize these nine substrates, although the activity levels were lower than those of PHs. The hepatic functions of hiPSC-hepa were further evaluated by examining the ability to uptake Indocyanine Green (ICG) and LDL (Fig. 4C and D, respectively). In addition to PHs, hiPSC-hepa had the ability to uptake ICG and to excrete ICG in a culture without ICG for 6 h (Fig. 4C), and to uptake LDL (Fig. 4D). These results suggest that hiPSC-hepa have enough CYP enzyme activity, conjugating enzyme activity, and hepatic transporter activity to metabolize various drugs.

To examine whether our hiPSC-hepa could be used to predict metabolism-mediated toxicity, hiPSC-hepa were incubated with Benzbromarone, which is known to generate toxic metabolites, and then cell viability was measured (Fig. 4E). Cell viability of hiPSC-hepa was decreased depending on the concentration of Benzbromarone. However, cell viability of hiPSC-hepa was much higher than that of PHs. To detect drug–induced cytotoxicity with high sensitivity in hiPSC-hepa, these cells were treated with Buthionine-SR-sulfoximine (BSO), which depletes cellular GST, and result in a decrease of cell viability of hiPSC-hepa as compared with that of non-treated cells (Fig. 4E). These results indicated that hiPSC-hepa would be more useful in drug screening under a condition of knockdown of conjugating enzyme activity.

Discussion

The establishment of an efficient hepatic differentiation technology from hESCs and hiPSCs would be important for the application of hESC-hepa and hiPSC-hepa to drug toxicity screening. Although we have previously reported that sequential transduc-

The cell viability of hiPSCs, hiPSC-hepa, PHs, and their BSO-treated cells (0.4 mM BSO was pre-treated for 24 h) was assessed by Alamar Blue assay after 48-hr exposure to differe2nt concentrations of benzbromarone. The cell viability is expressed as a percentage of that in cells treated only with solvent. All data are represented as mean ± SD (n = 3).

tion of SOX17, HEX, and HNF4α into hESC-derived cells could promote efficient hepatic differentiation [7], further hepatic maturation of the hESC-hepa and hiPSC-hepa was needed for this application. To further improve the differentiation efficiency of every step of hepatic differentiation (hESC to DE cells, DE cells to hepatoblasts, and hepatoblasts to hESC-hepa), we initially performed a screening of transcription factors. In the stage of DE differentiation, FOXA2 transduction could promote the most efficient DE differentiation (Fig. 1C). In the stage of hepatic commitment, expansion, and maturation, the combination of FOXA2 and HNF1α transduction strongly promoted hepatic commitment and maturation (Fig. 1F and J), although in the stage of hepatic expansion and maturation, HNF4α transduction was as efficient as that of HNF1α (Fig. 1J). Since HNF1α is one of the target genes of HNF4α [13], the signaling through HNF4α to HNF1α would be important for efficient hepatic expansion and maturation. Considering these results together, we ascertained a pair of two transcription factors, FOXA2 and HNF1α, that could promote efficient hepatic differentiation from hESCs. In embryogenesis, the expression of FOXA2 and HNF1α is initially detected in DE or hepatoblasts, respectively and the expression levels of both FOXA2 and HNF1α are elevated as the liver develops [14,15]. Therefore, our hepatic differentiation technology, which employs FOXA2 and HNF1α transduction, might mimic the gene expression pattern during embryogenesis.

We found that the gene expression levels of CYP enzymes, conjugating enzymes, hepatic transporters, and hepatic nuclear receptors were upregulated by FOXA2 and HNF1α transduction (Fig. 3D–G). In contrast to the high expression levels of hepatocyte-related genes, CYP induction potency and the drug metabolism capacity of our hiPSC-hepa were lower than those of PHs (Figs. 3I and 4A and B). One of the possible reasons for the difference between gene expression levels of CYP enzymes and CYP induction activity might be that there were insufficient expression levels of hepatic nuclear receptors (such as *PXR*, *SHR*, and *FXR*) in hiPSC-hepa (Fig. 3G). Because many CYPs require high expression levels of hepatic nuclear receptor for efficient drug metabolism [16], transduction of these hepatic nuclear receptor genes in hiPSC-hepa or development of a differentiation method that induces high expression of these nuclear receptors might improve the drug metabolic capacity. Another explanation for the low CYP activities in hiPSC-hepa, maybe that hiPSCs were established from an individual with low CYP activities; infact, it is known that large individual differences in CYP activities are observed among individuals. It might be important to use a hiPSC line established from a person with high CYP activities. It is essential to investigate the reasons behind this significant discordance, an issue that our group is currently planning to study.

In summary, our method, consisting of sequential FOXA2 and HNF1α transduction along with the addition of adequate soluble factors at each step of differentiation, is a valuable tool for the efficient generation of functional hepatocytes derived from hESCs and hiPSCs. The hiPSC-hepa exhibited a number of hepatocyte functions (such as ALB secretion, uptake of LDL or ICG, glycogen storage, and drug metabolism capacity). In addition, the hiPSC-hepa were successfully applied to the evaluation of drug-induced cytotoxicity. Therefore, the hESC-hepa and hiPSC-hepa might be used for drug screening in early phases of pharmaceutical development.

Conflict of interest

The authors who have taken part in this study declared that they do not have anything to disclose regarding funding or conflict of interest with respect to this manuscript.

Acknowledgements

We thank Misae Nishijima, Nobue Hirata, Miki Yoshioka, and Hiroko Matsumura for their excellent technical support. We thank Ms. Ong Tyng Tyng for critical reading of the manuscript. HM, MKF, and TH were supported by grants from the Ministry of Health, Labor, and Welfare of Japan. HM was also supported by Japan Research foundation For Clinical Pharmacology, The Nakatomi Foundation, and The Uehara Memorial Foundation. K. Kawabata was supported by Grants from the Ministry of Education, Sports, Science and Technology of Japan (20200076) and the Ministry of Health, Labor, and Welfare of Japan. K. Katayama and FS were supported by Program for Promotion of Fundamental Studies in Health Sciences of the National Institute of Biomedical Innovation (NIBIO).

Supplementary data

Supplementary data associated with this article can be found, in the online version, at http://dx.doi.org/10.1016/j.jhep.2012.04.038.

References

[1] Thomson JA, Itskovitz-Eldor J, Shapiro SS, Waknitz MA, Swiergiel JJ, Marshall VS, et al. Embryonic stem cell lines derived from human blastocysts. Science 1998;282:1145–1147.
[2] Takahashi K, Tanabe K, Ohnuki M, Narita M, Ichisaka T, Tomoda K, et al. Induction of pluripotent stem cells from adult human fibroblasts by defined factors. Cell 2007;131:861–872.
[3] Clayton DF, Darnell Jr JE. Changes in liver-specific compared to common gene transcription during primary culture of mouse hepatocytes. Mol Cell Biol 1983;3:1552–1561.
[4] Snykers S, De Kock J, Rogiers V, Vanhaecke T. In vitro differentiation of embryonic and adult stem cells into hepatocytes: state of the art. Stem cells 2009;27:577–605.
[5] Inamura M, Kawabata K, Takayama K, Tashiro K, Sakurai F, Katayama K, et al. Efficient generation of hepatoblasts from human ES cells and iPS cells by transient overexpression of homeobox gene HEX. Mol Ther 2011;19:400–407.
[6] Takayama K, Inamura M, Kawabata K, Tashiro K, Katayama K, Sakurai F, et al. Efficient and directive generation of two distinct endoderm lineages from human ESCs and iPSCs by differentiation stage-specific SOX17 transduction. PLoS One 2011;6:e21780.
[7] Takayama K, Inamura M, Kawabata K, Katayama K, Higuchi M, Tashiro K, et al. efficient generation of functional hepatocytes from human embryonic stem cells and induced pluripotent stem cells by HNF4alpha transduction. Mol Ther 2012;20:127–137.
[8] Duan Y, Ma X, Zou W, Wang C, Bahbahan IS, Ahuja TP, et al. Differentiation and characterization of metabolically functioning hepatocytes from human embryonic stem cells. Stem cells 2010;28:674–686.
[9] Furue MK, Na J, Jackson JP, Okamoto T, Jones M, Baker D, et al. Heparin promotes the growth of human embryonic stem cells in a defined serum-free medium. Proc Natl Acad Sci U S A 2008;105:13409–13414.
[10] Lacroix D, Sonnier M, Moncion A, Cheron G, Cresteil T. Expression of CYP3A in the human liver–evidence that the shift between CYP3A7 and CYP3A4 occurs immediately after birth. Eur J Biochem 1997;247:625–634.

[11] Nagata S, Toyoda M, Yamaguchi S, Hirano K, Makino H, Nishino K, et al. Efficient reprogramming of human and mouse primary extra-embryonic cells to pluripotent stem cells. Genes Cells 2009;14:1395–1404.
[12] Makino H, Toyoda M, Matsumoto K, Saito H, Nishino K, Fukawatase Y, et al. Mesenchymal to embryonic incomplete transition of human cells by chimeric OCT4/3 (POU5F1) with physiological co-activator EWS. Exp Cell Res 2009;315:2727–2740.
[13] Gragnoli C, Lindner T, Cockburn BN, Kaisaki PJ, Gragnoli F, Marozzi G, et al. Maturity-onset diabetes of the young due to a mutation in the hepatocyte nuclear factor-4 alpha binding site in the promoter of the hepatocyte nuclear factor-1 alpha gene. Diabetes 1997;46:1648–1651.
[14] Ang SL, Wierda A, Wong D, Stevens KA, Cascio S, Rossant J, et al. The formation and maintenance of the definitive endoderm lineage in the mouse: involvement of HNF3/forkhead proteins. Development 1993;119: 1301–1315.
[15] Kyrmizi I, Hatzis P, Katrakili N, Tronche F, Gonzalez FJ, Talianidis I. Plasticity and expanding complexity of the hepatic transcription factor network during liver development. Genes Dev 2006;20:2293–2305.
[16] Lehmann JM, McKee DD, Watson MA, Willson TM, Moore JT, Kliewer SA. The human orphan nuclear receptor PXR is activated by compounds that regulate CYP3A4 gene expression and cause drug interactions. J Clin Invest 1998;102:1016–1023.

Supplemental figure 1

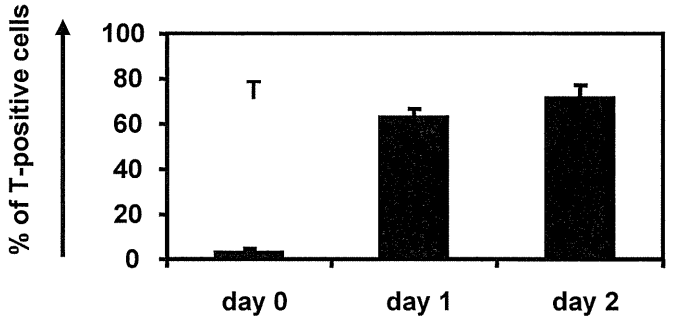

Fig. S1 The formation of mesendoderm cells from hESCs

hESCs (H9) were differentiated as described in **Figure 2A** and subjected to immunostaining with anti-T antibodies on day 0, 1, or 2. The percentage of antigen-positive cells was measured by FACS analysis. All data are represented as means ± SD (*n*=3).

Supplemental figure 2

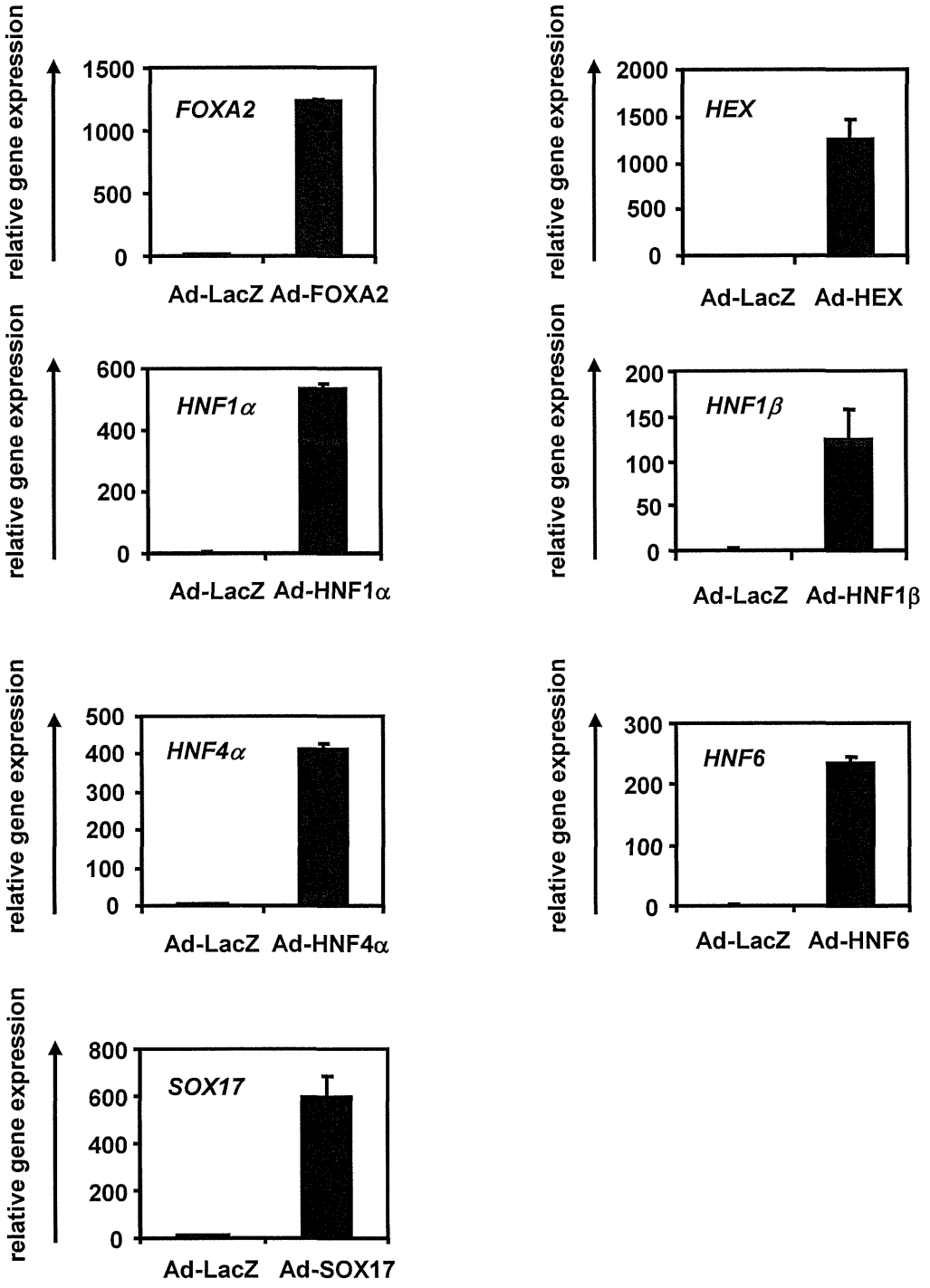

Fig. S2 Overexpression of FOXA2, HNF1 α, HNF4 α, SOX17, HEX, HNF1 β, or HNF6 mRNA in mesendoderm cells by Ad- FOXA2, Ad-HNF1 α, Ad-HNF4 α, Ad-SOX17, Ad-HEX, Ad-HNF1 β, or Ad-HNF6 transduction, respectively

hESCs (H9) were differentiated into mesendoderm cells (day 2) as described in **Figure 2A** and were transduced with 3,000 VP/cells of Ad-FOXA2, Ad-HNF1 α, Ad-HNF4 α, Ad-SOX17, Ad-HEX, Ad-HNF1 β, or Ad-HNF6 for 1.5 hr. On day 4, real-time RT-PCR analysis of *FOXA2*, *HNF1 α*, *HNF4 α*, *SOX17*, *HEX*, *HNF1 β*, or *HNF6* expression was performed in Ad-FOXA2-, Ad-HNF1 α-, Ad-HNF4 α-, Ad-SOX17-, Ad-HEX-, Ad-HNF1 β-, or Ad-HNF6-transduced cells, respectively. On the y axis, the gene expression levels of *FOXA2*, *HNF1 α*, *HNF4 α*, *SOX17*, *HEX*, *HNF1 β*, or *HNF6* in Ad-LacZ-transduced cells on day 4 were taken as 1.0. All data are represented as means $\pm$ SD (n=3).

Supplemental figure 3

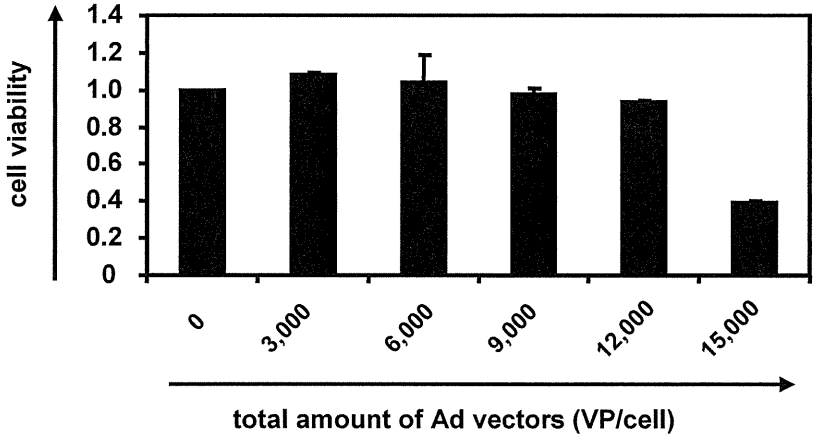

Fig. S3 Optimization of the amount of Ad vectors to transduce

hESC (H9)-derived cells were transduced with 750, 1,500, 2250, 3,000, or 3,750 VP/cell of Ad-LacZ for 1.5 hr on day 2, 6, 9, and 12, and then cultured as described in **Figure 2A.** On day 20, the cell viability was evaluated with Alamar Blue assay. The horizontal axis represents the total amount of Ad vector (3,000, 6,000, 9,000, 12,000, or 15,000 VP/cell, respectively). On the y axis, the level of non-transduced cells was defined as 1.0. All data are represented as means ± SD (*n*=3).

Supplemental figure 4

A

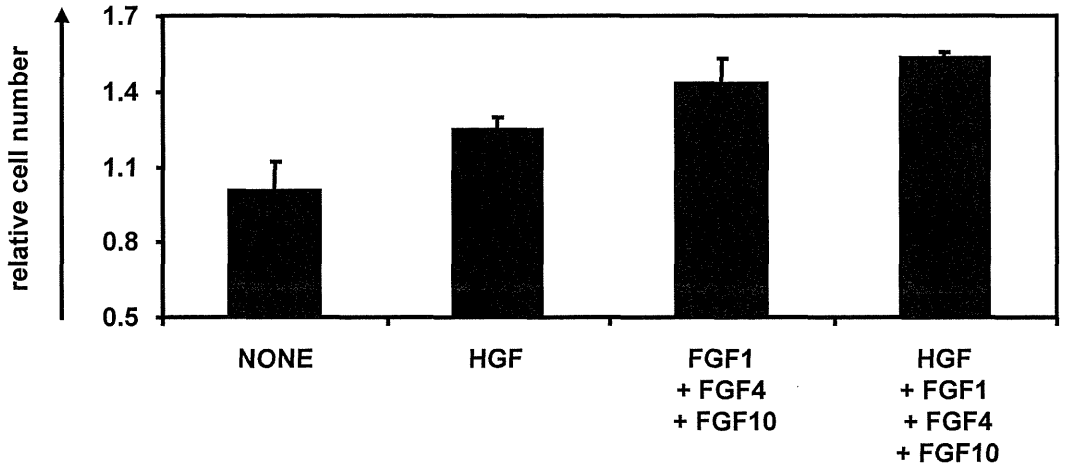

B

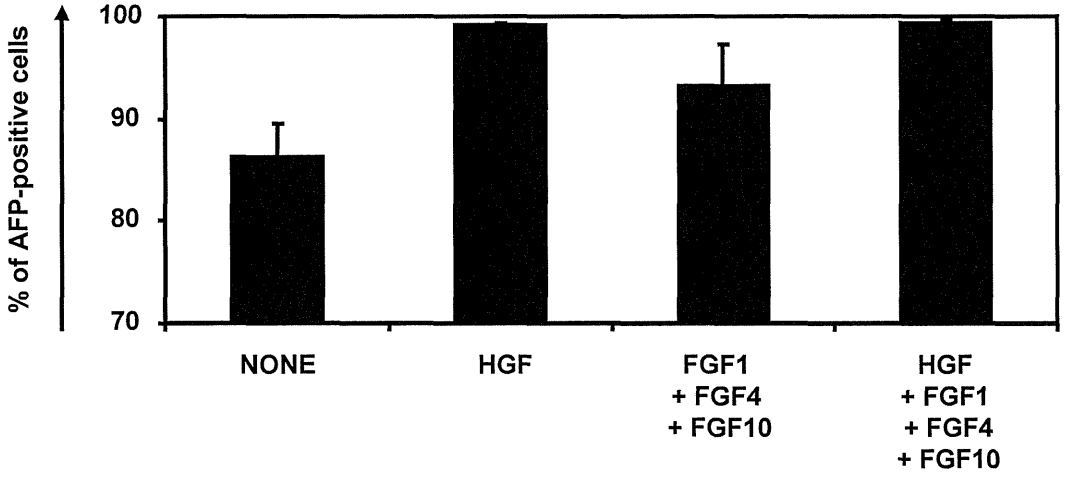

Fig. S4 Expansion of the hepatoblast population by HGF, FGF1, FGF4, and HGF stimulation
hESCs (H9) were differentiated into hepatoblasts as described in **Figure 2A.** The hepatoblasts (day 9) were cultured with the HCM without additional growth factors (NONE), the HCM containing HGF, the HCM containing FGF1 + FGF4 + FGF10, or the HCM containing HGF + FGF1 + FGF4 + FGF10. The concentration of the growth factors used in this experiment was 10 ng/ml. (A) After the hepatoblasts (day 9) were cultured with the medium containing various growth factors (no additional growth factors, addition of HGF, addition of FGF1 + FGF4 + FGF10, or addition of HGF + FGF1 + FGF4 + FGF10) for 3 days, the number of the cells was counted on day 12. The cell number of untreated population was taken as 1.0. (B) On day 12, the cells were subjected to immunostaining with anti-AFP antibodies. The percentage of antigen-positive cells was measured by FACS analysis. All data are represented as means ± SD (n=3). The results showed that addition of HGF, FGF1, FGF4, and FGF10 increased the number of the hepatoblasts.

Supplemental figure 5

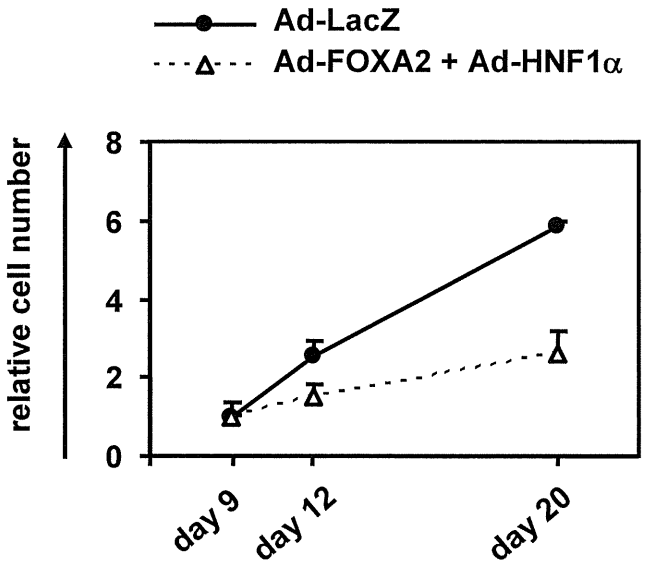

Fig. S5 Arrest of hepatoblast proliferation by FOXA2 and HNF1 α transduction.

hESCs were differentiated into the hepatoblasts (day 9) according to the protocol described in **Figure 2A**, and then transduced with 3,000 VP/cell of Ad-LacZ or 1,500 VP/cell of each Ad-FOXA2 and Ad-HNF1 α for 1.5 hr on day 9 and 12 and cultured until day 20 according to the protocol described in Figure 2A. The cells were not passaged on day 11. The cell number was counted on day 9, 12, and 20 of differentiation. The cell number on day 9 was taken as 1.0. All data are represented as means $\pm$ SD (n = 3).

Supplemental figure 6

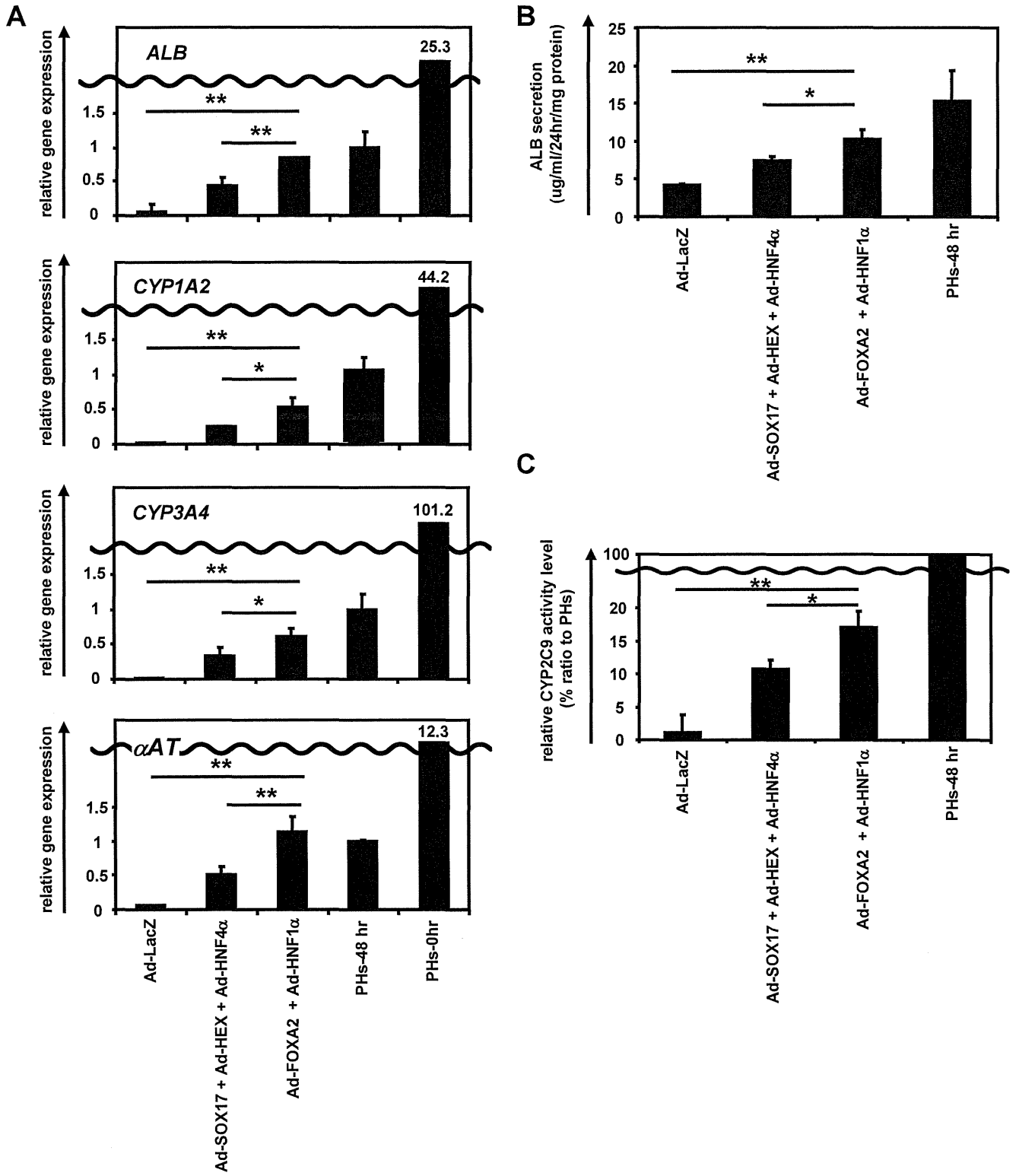

Fig. S6 FOXA2 and HNF1 α transduction promote more efficient hepatic differentiation as compared with SOX17, HEX, and HNF4 α transduction

hiPSCs (Dotcom) were differentiated into hepatocytes as described in **Figure 2A.** (A) On day 20, the gene expression levels of *ALB*, *CYP1A2*, *CYP3A4*, and *αAT* were examined by real-time RT-PCR in Ad-LacZ-transduced cells (Ad-LacZ), Ad-SOX17-, Ad-HEX-, and Ad-HNF4 α-transduced cells (Ad-SOX17 + Ad-HEX + Ad-HNF4 α), Ad-FOXA2- and Ad-HNF1 α-transduced cells (Ad-FOXA2 + Ad-HNF1 α), PHs cultured for 48 hr after plated (PHs-48hr), and PHs collected immediately after thawing (PHs-0hr). On the y axis, the gene expression levels of *ALB*, *CYP1A2*, *CYP3A4*, and *αAT* in PH-48hr were taken as 1.0. (B) The amount of ALB secretion was examined by ELISA in Ad-LacZ, Ad-SOX17 + Ad-HEX + Ad-HNF4 α, Ad-FOXA2 + Ad-HNF1 α, PHs-48hr, and PH-0hr. (C) The CYP2C9 activity level was examined in Ad-LacZ, Ad-SOX17 + Ad-HEX + Ad-HNF4 α, Ad-FOXA2 + Ad-HNF1 α, PHs-48hr, and PH-0hr. On the y axis, the CYP2C9 activity levels in PH-48hr were taken as 1.0. All data are represented as means ± SD (*n*=3).

Supplemental figure 7

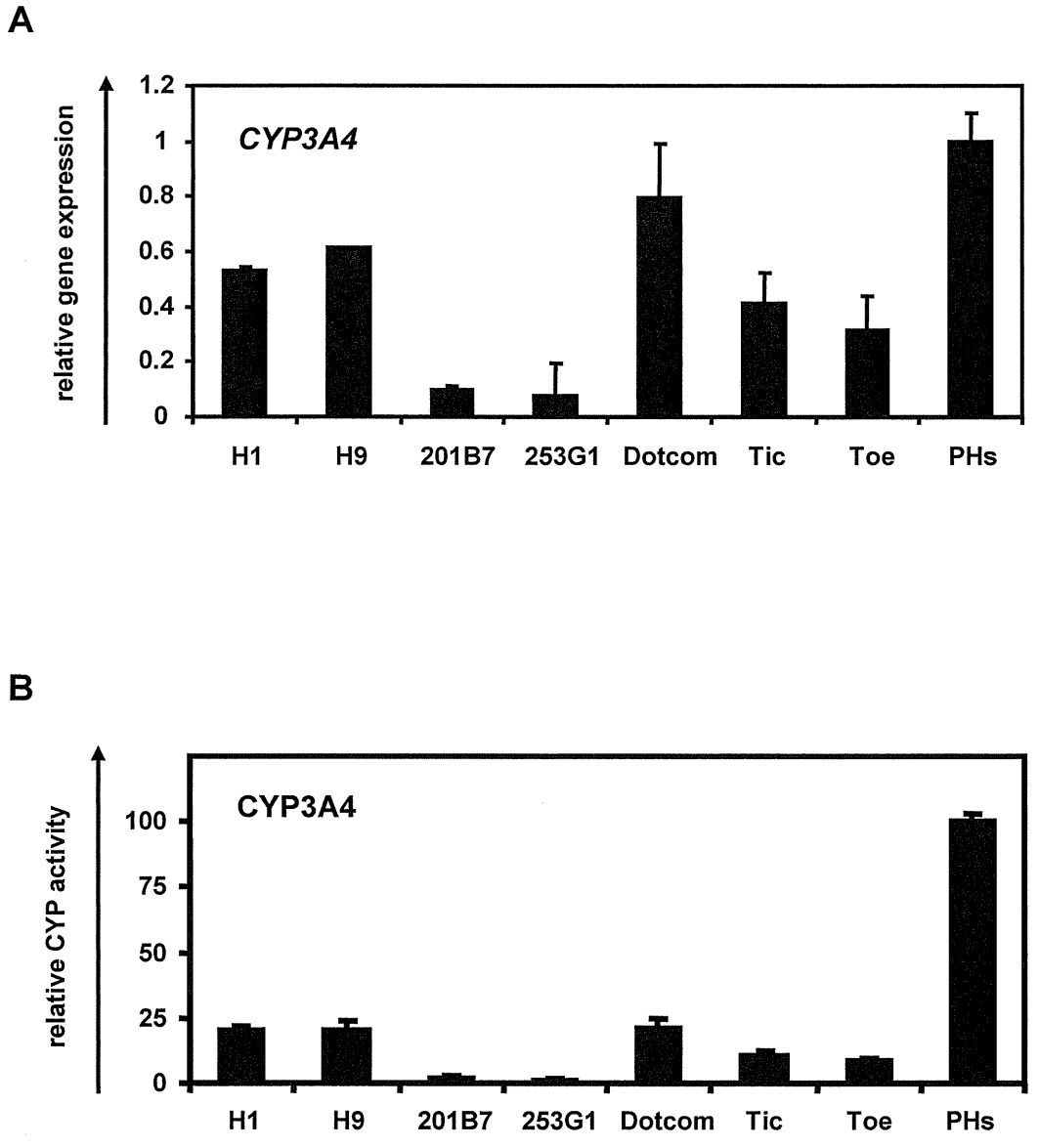

Fig. S7 Comparison of the hepatic differentiation capacity of various hESC and hiPSC lines

hESCs (H1 and H9) and hiPSCs (201B7, 253G1, Dotcom, Tic, and Toe) were differentiated into hepatocyte-like cells as described in **Figure 2A.** (A) On day 20, the gene expression level of *CYP3A4* was examined by real-time RT-PCR. On the y axis, the gene expression level of *CYP3A4* in PHs, which were cultured for 48 hr after the cells were plated, was taken as 1.0. (B) On day 20, the CYP3A4 activity level was examined by using a P450-GloTM CYP3A4 Assay Kit. On the y axis, the CYP3A4 activity levels in PHs were taken as 100. All data are represented as means ± SD (n=3).

Supplemental figure 8

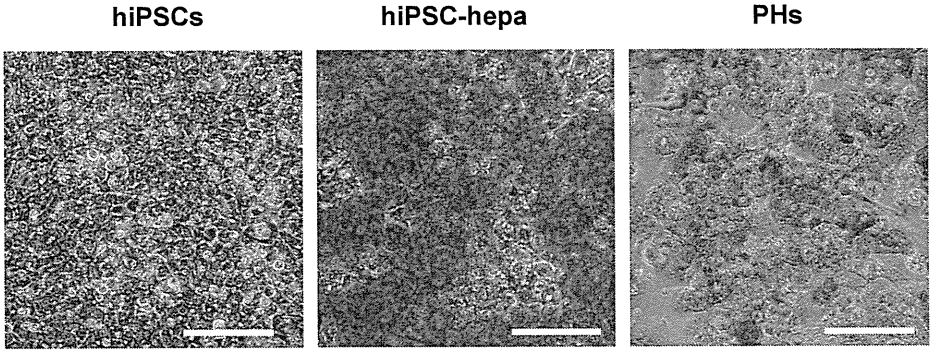

Fig. S8 Storage of glycogen in hiPSC-hepa

hiPSCs (Dotcom) were differentiated into hepatocytes as described in **Figure 2A.** Glycogen storage of hiPSCs, hiPSC-hepa, and PHs, which were cultured for 48 hr after the cells were plated, was assessed by Periodic Acid-Schiff (PAS) staining. PAS staining was performed on day 20 of differentiation. Glycogen storage is indicated by pink or dark red-purple cytoplasms. The scale bars represent 50 μm.

Supplemental figure 9

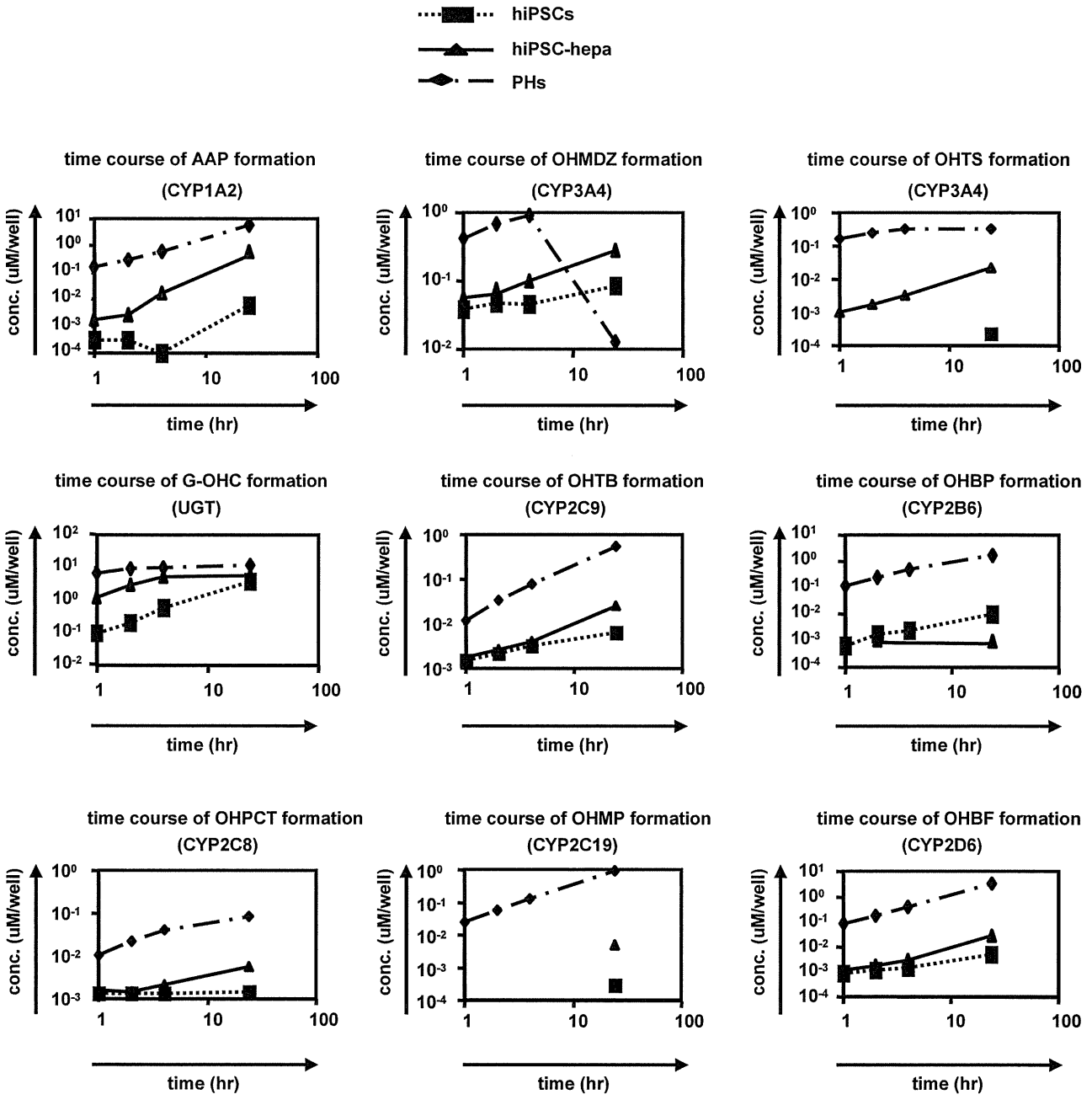

Fig. S9 The time course of metabolites formation in hiPSCs, hiPSC-hepa, or PHs

hiPSCs (Dotcom) were differentiated into hepatocytes as described in **Figure 2A.** Quantitation of metabolites in hiPSCs, hiPSC-hepa, and PHs treated with nine substrates (Phenacetin [PHE], Bupropion [BP], Paclitazel [PCT], Tolbutamide [TB], *S*-mephenytoin [MP], Bufuralol [BF], Midazolam [MDZ], Testosterone [TS], and Hydroxyl coumarin [OHC]) was performed. Supernatants were collected at 1, 2, 4, or 24 hr after incubation with each substrate, which were the probes for CYP1A2, 2B6, 2C8, 2C9, 2C19, 2D6, 3A4, 3A4 and UGT, respectively. The quantity of metabolites (Acetaminophen [AAP], Hydroxybupropion [OHBP], 6α-hydroxypaclitaxel [OHPCT], Hydroxytolbutamide [OHTB], 4'-hydroxymephenytoin [OHMP], 1'-hydroxybufuralol [OHBF], 1'-hydroxymidazolam [OHMDZ], 6β-hydroxytestosterone [OHTS], 7-Hydroxycoumarin glucuronide [G-OHC], respectively) was measured by LC-MS/MS. The substrates and that metabolites used in this study are summarized in **Table S5.** All data are represented as means ± SD (n=3).

Supplemental Materials and Methods

hESCs and hiPSCs culture

Two hESC lines, H1 and H9 (WiCell Research Institute), were maintained on a feeder layer of mitomycin C-treated mouse embryonic fibroblasts (Millipore) with Repro Stem (ReproCELL) supplemented with 5 ng/ml fibroblast growth factor 2 (FGF2) (Sigma). H1 and H9 were used following the Guidelines for Derivation and Utilization of Human Embryonic Stem Cells of the Ministry of Education, Culture, Sports, Science and Technology of Japan.

Three human iPSC lines generated from the human embryonic lung fibroblast cell line MCR5 were provided from the JCRB Cell Bank (Tic, JCRB Number: JCRB1331; Dotcom, JCRB Number: JCRB1327; Toe, JCRB Number: JCRB1338) [1, 2]. These human iPSC lines were maintained on a feeder layer of mitomycin C-treated mouse embryonic fibroblasts with iPSellon (Cardio) supplemented with 10 ng/ml FGF2. Other human iPSC lines, 201B7 and 253G1, were generated from human dermal fibroblasts (HDF) was kindly provided by Dr. S. Yamanaka (Kyoto University) [3]. The human iPSC lines, 201B7 and 253G1, were maintained on a feeder layer of mitomycin C-treated mouse embryonic fibroblasts with Repro Stem (Repro CELL) supplemented with 5 ng/ml FGF2 (Sigma).

Adenovirus (Ad) vectors

Ad vectors were constructed by an improved *in vitro* ligation method [4, 5]. The human HNF1α, FOXA2, and HNF6 gene (accession number NM_000545, NM_021784, and NM_004498, respectively) were amplified by PCR using primers: HNF1α Fwd 5'-GATCTCTAGACTGTGGCAGCCGAGAG-3' and HNF1α Rev 5'-CTAAGGAATTCCCTGCTATCTTGAGGTCCTGGTC -3'; FOXA2 Fwd 5'-AAAGAATTCACTGCCATGCACTCGGCTTCCAG-3' and FOXA2 Rev 5'-CCTGCAACAACAGCAATGGAGGAGAAC -3'; HNF6 Fwd 5'-CATCCTCGAGGTGTCCGCCGCCTGCTC-3' and HNF6 Rev 5'-CTAAGGAATTCCCTGCTATCTTGAGGTCCTGGTC -3'. The human HNF1β gene (accession number BC_017714) was purchased from Excellgen. The human HNF1α, FOXA2, or HNF6 gene was inserted into pBSKII (Invitrogen), resulting in pBSKII-HNF1α, -FOXA2, or -HNF6, respectively. Then, the human HNF1α, HNF1β, FOXA2, or HNF6 gene was inserted into pHMEF5 [6], which contains the human

elongation factor-1α (EF-1α) promoter, resulting in pHMEF-HNF1α, -HNF1β, -FOXA2, or -HNF6, respectively. The pHMEF-HNF1α, -HNF1β, -FOXA2, or -HNF6 was digested with I-CeuI/PI-SceI and ligated into I-CeuI/PI-SceI-digested pAdHM41-K7 [7], resulting in pAd-HNF1α, -HNF1β, -FOXA2, or -HNF6, respectively. The human EF-1α promoter-driven LacZ-, SOX17-, HEX-, HNF4α-expressing Ad vectors (Ad-LacZ, Ad-SOX17, Ad-HEX, or Ad-HNF4α, respectively) were constructed previously [8-10]. All of Ad vectors contain a stretch of lysine residue (K7) peptides in the C-terminal region of the fiber knob for more efficient transduction of hESCs, hiPSCs, and DE cells, in which transfection efficiency was almost 100%, and purified as described previously [8, 10, 11]. The vector particle (VP) titer was determined by using a spectrophotometric method [12].

Flow cytometry

Single-cell suspensions of hESCs, hiPSCs, and their derivatives were fixed with methanol at 4°C for 20 min and then incubated with the primary antibody described in **Table S2**, followed by the secondary antibody. Flow cytometry analysis was performed using a FACS LSR Fortessa flow cytometer (BD biosciences).

RNA isolation and reverse transcription-polymerase chain reaction (RT-PCR)

Total RNA was isolated from hESCs, hiPSCs, and their derivatives using ISOGENE (Nippon Gene). cDNA was synthesized using 500 ng of total RNA with a Superscript VILO cDNA synthesis kit (Invitrogen). Real-time RT-PCR was performed with Taqman gene expression assays (Applied Biosystems) or SYBR Premix Ex Taq (TaKaRa) using an ABI PRISM 7000 Sequence Detector (Applied Biosystems). Relative quantification was performed against a standard curve and the values were normalized against the input determined for the housekeeping gene, glyceraldehyde 3-phosphate dehydrogenase (GAPDH). The primer sequences used in this study are described in **Table S3**.

Immunohistochemistry

The cells were fixed with methanol or 4% paraformaldehyde (PFA) (Wako). After blocking with PBS containing 2% BSA (Sigma) and 0.2% Triton X-100 (Sigma), the cells were incubated with primary antibody at 4°C for 16 hr, followed by incubation

with a secondary antibody that was labeled with Alexa Fluor 488 (Invitrogen) or Alexa Fluor 594 (Invitrogen) at room temperature for 1 hr. All the antibodies are listed in **Table S2**.

ELISA

The hiPSCs were differentiated into hepatocytes as described in **Figure 2A**. The culture supernatants, which were incubated for 24 hr after fresh medium was added, were collected and analyzed for the amount of ALB secretion by ELISA. ELISA kits for ALB were purchased from Bethyl. ELISA was performed according to the manufacturer's instructions. The amount of ALB secretion was calculated according to each standard followed by normalization to the protein content per well.

Urea secretion

The hiPSCs were differentiated into hepatocytes as described in **Figure 2A**. The culture supernatants, which were incubated for 24 hr after fresh medium was added, were collected and analyzed for the amount of urea secretion. Urea measurement kits were purchased from BioAssay Systems. The experiment was performed according to the manufacturer's instructions. The amount of urea secretion was calculated according to each standard followed by normalization to the protein content per well.

CYP induction

To measure CYP1A2, 2B6, and 3A4 induction potency, real-time RT-PCR was performed. The undifferentiated hiPSCs, hiPSC-hepa, and PHs were treated with b-naphthoflavone [bNF], phenobarbital [PB], or rifampicin [RIF], which is an inducer for CYP1A2, 2B6, or 3A4, at a final concentration of 10 μM, 750 μM, or 10 μM, respectively, for 48 hr. The CYP inducers used in this study are summarized in **Table S4**. Controls were treated with DMSO (final concentration 0.1%). Inducer compounds were replaced daily.

Drug metabolism capacity of hiPSC-hepa

All hiPSCs, hiPSC-hepa, and PHs were treated with Phenacetin [PHE], Bupropion [BP], Paclitaxel [PCT], Tolbutamide [TB], *S*-mephenytoin [MP], Bufuralol [BF], Midazolam

[MDZ], Testosterone [TS], and Hydroxyl coumarin [OHC] at a working concentration of 10 μM for PHE, 150 μM for BP, 20 μM for PCT, 500 μM for TB, 200 μM for MP, 50 μM for BF, 10 μM for MDZ, 100 μM for TS, and 10 μM for OHC in the medium. The substrates (PHE, BP, PCT, TB, MP, BF, MDZ, RS, and OHC) and that metabolites (Acetaminophen [AAP], Hydroxybupropion [OHBP], 6α-hydroxypaclitaxel [OHPCT], Hydroxytolbutamide [OHTB], 4'-hydroxymephenytoin [OHMP], 1'-hydroxybufuralol [OHBF], 1'-hydroxymidazolam [OHMDZ], 6β-hydroxytestosterone [OHTS], 7-Hydroxycoumarin glucuronide [G-OHC]), which are used in this study, are summarized in **Table S5**. The cocktail assays were adopted for group 1; PHE and MDZ and group 2; PCT, TB, MP and BF. The other substrates were incubated alone. The supernatant was collected at 1, 2, 4, and 24 hr respectively after treatment, and immediately mixed with two volumes of acetonitrile and methanol (1:1, v/v) containing 50 μM of dextrophan and 50 μM of propranolol as internal standards. Samples were filtrated with MutiScreen (Nihon Millipore K.K.) for 5 min at 1750 *g*, and an aliquot (5 μl) of the supernatant was analyzed by liquid chromatography tandem mass spectrometry (LC-MS/MS) to determine the concentration of metabolite quantitatively according to each standard curve. The LC-MS/MS system consisting of a Prominence HPLC system (Shimadzu Corporation) and an API 5000 triple quadrupole mass spectrometer (AB SCIEX) with an L-Column ODS (150 mm x 2.1 mm i.d., 5 μm; Chemicals Evaluation and Research Institute) was used. The mass spectrometer was set to the multiple-reaction monitoring mode and was operated with the electrospray ionization source in positive ion mode. The mobile phase was delivered at a flow rate of 0.5 ml/min using a gradient elution profile consisting of solvent A (0.02% formic acid/distilled water) and solvent B (0.02% formic acid/ acetonitrile). The details of the LC gradient conditions and mass spectrometer conditions are described in **Tables S6** and **S7**, respectively. The concentrations of each metabolite were calculated according to each standard followed by normalization to the protein content per well.

Primary human hepatocytes

In **Figures 3C, 4C, 4D, 4E** and **S8**, one lot of cryopreserved human hepatocytes (lot Hu8072 [CellzDirect]) was used. In **Figure 1, 3A, 3B, 3D-3H, S6,** and **S7**), three lots of cryopreserved human hepatocytes (lot Hu8072 [CellzDirect], HC2-14, and HC10-101 [Xenotech]) were used. These three lots of crypreserved human hepatocytes (lot Hu8072 [CellzDirect], HC2-14, and HC10-101 [Xenotech]) were cultured according to our previous report [11]. In **Figures 3I, 4A, 4C** and **S9**, three

lots of cryopreserved human hepatocytes (lot HH309, HEP187087 [Tissue Transformation Technologies], and Hu1126 [CellzDirect]) were used. The vials of hepatocytes were rapidly thawed in a shaking water bath at 37°C; the contents of the vial were emptied into prewarmed Williams' medium E (Sigma) and the suspension was centrifuged at 100*g* for 5 min at room temperature. The hepatocyte pellet was resuspended in 2.0 ml of prewarmed Williams' medium E by gentle inversion, and the cell number and viability were assessed using the trypan blue exclusion test. The hepatocytes were seeded at $2.5x10^5$ cells/well in Williams' medium E onto a collagen-coated 24-well plate. The medium was replaced with Hepato-STIM (BD Biosciences) after 24 hr after seeding and then changed daily. The hepatocytes were subjected to inducer treatment at 48 hr after cell seeding.

Cell Viability Tests

Cell viability was assessed by using an Alamar Blue assay kit (Biosource). The culture medium was replaced with culture medium containing 0.5 mg/ml solution of Alamar Blue and the cells were incubated for 3 hr at 37°C. The supernatants of the cells were measured at a wavelength of 570 nm with background subtraction at 600 nm in a plate reader. Control refers to incubations in the absence of test compounds and was considered as 100% viability value. In the case of Buthionine-SR-sulfoximine (BSO) addition, the cells were pre-treated with BSO for 24 hr.

Assay for Cytochrome P450 Activity

To measure the cytochrome P450 3A4 and 2C9 activity of the cells, we performed Lytic assays by using a P450-GloTM CYP3A4 and 2C9 Assay Kit (Promega) in **Supplemental figures 6C** and **7B**. We measured the fluorescence activity with a luminometer (Lumat LB 9507; Berthold) according to the manufacturer's instructions.

Cellular Uptake and Excretion of Indocyanine Green

Indocyanine Green (ICG) (Sigma) was dissolved in DMSO at 100 mg/ml, then added to a culture medium of the hepatocyte-like cells to a final concentration of 1 mg/ml on day 20. After incubation at 37°C for 60 min, the medium with ICG was discarded and the cells were washed with PBS. The cellular uptake of ICG was then examined by microscopy. PBS was then replaced by the culture medium and the cells

were incubated at 37°C for 6 hr. The excretion of ICG was examined by microscopy.

Uptake of LDL

The cells were cultured with medium containing Alexa-488-labeled LDL (Invitrogen) for 1 hr, and then the cells that could uptake LDL were assessed by immunohistochemistry and FACS analysis.

Periodic Acid-Schiff (PAS) Assay for Glycogen

The cells were fixed with 4% PFA and stained using a PAS staining system (Sigma) on day 20 of differentiation according to the manufacturer's instructions.

Supplemental figure legends

Fig. S1 The formation of mesendoderm cells from hESCs

hESCs (H9) were differentiated as described in **Figure 2A** and subjected to immunostaining with anti-T antibodies on day 0, 1, or 2. The percentage of antigen-positive cells was measured by FACS analysis. All data are represented as means ± SD (n=3).

Fig. S2 Overexpression of FOXA2, HNF1α, HNF4α, SOX17, HEX, HNF1β, or HNF6 mRNA in mesendoderm cells by Ad- FOXA2, Ad-HNF1α, Ad-HNF4α, Ad-SOX17, Ad-HEX, Ad-HNF1β, or Ad-HNF6 transduction, respectively

hESCs (H9) were differentiated into mesendoderm cells (day 2) as described in **Figure 2A** and were transduced with 3,000 VP/cells of Ad-FOXA2, Ad-HNF1α, Ad-HNF4α, Ad-SOX17, Ad-HEX, Ad-HNF1β, or Ad-HNF6 for 1.5 hr. On day 4, real-time RT-PCR analysis of *FOXA2*, *HNF1α*, *HNF4α*, *SOX17*, *HEX*, *HNF1β*, or *HNF6* expression was performed in Ad-FOXA2-, Ad-HNF1α-, Ad-HNF4α-, Ad-SOX17-, Ad-HEX-, Ad-HNF1β-, or Ad-HNF6-transduced cells, respectively. On the y axis, the gene expression levels of *FOXA2*, *HNF1α*, *HNF4α*, *SOX17*, *HEX*, *HNF1β*, or *HNF6* in Ad-LacZ-transduced cells on day 4 were taken as 1.0. All data are represented as means ± SD (n=3).

Fig. S3 Optimization of the amount of Ad vectors to transduce

hESC (H9)-derived cells were transduced with 750, 1,500, 2250, 3,000, or 3,750 VP/cell of Ad-LacZ for 1.5 hr on day 2, 6, 9, and 12, and then cultured as described in **Figure 2A**. On day 20, the cell viability was evaluated with Alamar Blue assay. The horizontal axis represents the total amount of Ad vector (3,000, 6,000, 9,000, 12,000, or 15,000 VP/cell, respectively). On the y axis, the level of non-transduced cells was defined as 1.0. All data are represented as means ± SD (n=3).

Fig. S4 Expansion of the hepatoblast population by HGF, FGF1, FGF4, and HGF stimulation

hESCs (H9) were differentiated into hepatoblasts as described in **Figure 2A**. The hepatoblasts (day 9) were cultured with the HCM without additional growth factors (NONE), the HCM containing HGF, the HCM containing FGF1 + FGF4 + FGF10, or the HCM containing HGF + FGF1 + FGF4 + FGF10. The concentration of the growth factors used in this experiment was 10 ng/ml. (**A**) After the hepatoblasts (day 9) were cultured with the medium containing various growth factors (no additional growth factors, addition of HGF, addition of FGF1 + FGF4 + FGF10, or addition of HGF + FGF1 + FGF4 + FGF10) for 3 days, the number of the cells was counted on day 12. The cell number of untreated population was taken as 1.0. (**B**) On day 12, the cells were subjected to immunostaining with anti-AFP antibodies. The percentage of antigen-positive cells was measured by FACS analysis. All data are represented as means ± SD (n=3). The results showed that addition of HGF, FGF1, FGF4, and FGF10 increased the number of the hepatoblasts.

Fig. S5 Arrest of hepatoblast proliferation by FOXA2 and HNF1α transduction.

hESCs were differentiated into the hepatoblasts (day 9) according to the protocol described in **Figure 2A**, and then transduced with 3,000 VP/cell of Ad-LacZ or 1,500 VP/cell of each Ad-FOXA2 and Ad-HNF1α for 1.5 hr on day 9 and 12 and cultured until day 20 according to the protocol described in **Figure 2A**. The cells were not passaged on day 11. The cell number was counted on day 9, 12, and 20 of differentiation. The cell number on day 9 was taken as 1.0. All data are represented as means ± SD (n = 3).

Fig. S6 FOXA2 and HNF1α transduction promote more efficient hepatic differentiation as compared with SOX17, HEX, and HNF4α transduction

hiPSCs (Dotcom) were differentiated into hepatocytes as described in **Figure 2A**.